

# Crack Paths from Weld Details in Three-dimensional Plate Structures

Y. Sumi and T. Okawa

Department of Systems Design for Ocean-Space, Yokohama National University  
79-5 Tokiwadai, Hodogaya-ku, Yokohama 240-8501, Japan  
[sumi@structlab.shp.ynu.ac.jp](mailto:sumi@structlab.shp.ynu.ac.jp)

***ABSTRACT.** In the present paper, a simulation program is developed for multiple fatigue cracks propagating in a three-dimensional stiffened panel structure, where it can predict fatigue crack lives and paths by taking into account of the interaction of multiple cracks, load shedding during crack propagation and welding residual stress. Various fatigue crack propagations in longitudinal stiffeners of ship structures are investigated by both the present simulation method and experiments. From these results, it is found that the crack propagation may considerably change, depending on the loading conditions, structural details and residual stress distributions. This means that one could possibly manage to avoid fatal damage of the skin-plate by properly designing the structural details.*

## INTRODUCTION

Usually, fatigue cracks are detected by surveyor's visual inspection. Although fatigue cracks are preferred to be detected at an earlier stage, small cracks such as those illustrated in Fig.1 (a) may sometimes be overlooked because of the poor accessibility and visibility. In contrast, the long fatigue cracks such as those in Figs.1 (b) and (c) may be easily detected by visual inspection, but their remaining lives generally make up just a few percent of the total lives. If one can utilize the several favorable effects to retard the propagation rate and also to avoid hazardous crack propagation, a rational fatigue crack management as illustrated in Fig.2 could be applied, where the fatigue crack propagation behavior should be predicted accurately so as to manage the periodical inspections of fatigue cracks of visible size at least once or twice during the service life (see Ref.[1]).

In our previous studies, Sumi and his associates have developed a simulation program, "CP-System," for a fatigue crack propagating in a welded plate structure, which can predict fatigue crack lives and paths [2-5]. In the simulation program, "through-the-thickness" crack propagation is formulated as a two-dimensional in-plane problem, and the crack propagation behavior is simulated by step-by-step finite element analyses. In order to simulate the realistic fatigue crack propagation in large-scale structures, the super-element technique is utilized, and the influencing factors such as

geometry of structural details, load shedding during crack propagation, and welding residual stress are taken into consideration. It has been confirmed that the simulation program can reasonably estimate the fatigue crack propagation lives in welded plate structures, however, several issues still exist to be solved;

- the problem of multiple cracks simultaneously propagating in a three-dimensional stiffened panel structure (i.e. the crack propagation in Fig.1 (b) ),
- reduction of computation time.

Having improved the equation solver for the reduction of computation time, a simulation method is developed for simultaneously propagating multiple cracks. It is then applied to the fatigue crack propagation at the connection of longitudinal stiffeners and transverse girders. In the numerical simulations, various aspects are considered such as the loading conditions, the structural details of longitudinal and transverse connections, and the welding residual stress. Finally, the numerical results are compared with full-scale fatigue tests.

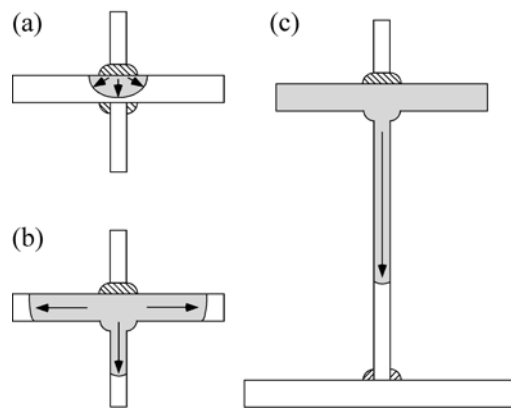


Figure 1 Fatigue crack propagation in a longitudinal stiffener; (a) surface crack at the weld toe, (b) through-the-thickness crack in the face-plate and the web-plate, (c) through-the-thickness crack in the web-plate.

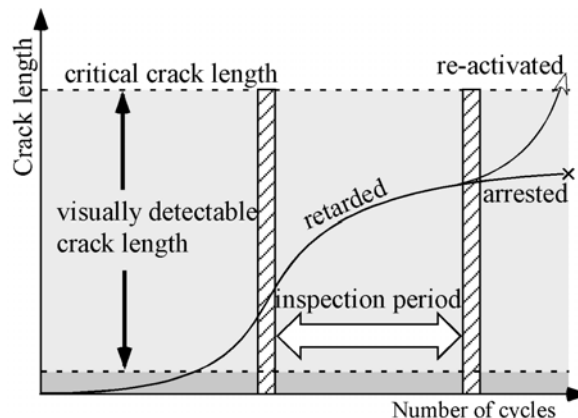


Figure 2 Proposed concept of fatigue crack management in a welded structure.

## MULTIPLE CRACKS SIMULTANEOUSLY PROPAGATING IN A THREE-DIMENSIONAL STIFFENED STRUCTURE

Let us consider a thin plate structure as shown in Fig.3, which consists of thin plates containing multiple cracks. The structure is divided into  $M$  subdomains,  $\Omega_l$  ( $l=1, \dots, M$ ), in which there exists no more than one crack tip. An orthogonal coordinate system is defined in each subdomain. Body force,  $f_i^l$ , is prescribed in the subdomain  $\Omega_l$ . Surface traction,  $t_i^l$ , is prescribed on the outer boundary,  $S_t^l$ , and on the crack surface,  $S_c^l$ . Surface displacement,  $v_i^l$ , is prescribed on the outer boundary  $S_u^l$ . The boundary of the subdomain  $\Omega_l$  is denoted by  $\Gamma_l$  and the interface between the subdomain  $\Omega_l$  and its neighboring subdomain  $\Omega_n$  is denoted by  $\Gamma_l \cap \Gamma_n$ .

In the present formulation the three-dimensional compatibility conditions and the equilibrium conditions are introduced along the interfaces of subdomains, respectively. In the developed finite element program, these conditions are satisfied by connecting each neighboring subdomain by using rigid bar elements with zero-length. With regard to the finite element modeling in the crack propagating domains, the membrane element is employed because the effect of the local out-of-plane bending component is sufficiently small in the problem treated in this study.

The simulation program was developed in order to deal with multiple cracks propagating in a three-dimensional structure. The main procedure of the simulation is summarized as follows (see Fig.4);

1. finite element mesh is automatically generated by an advanced paving method [6] in each crack-propagating domain, while a super-element is generated to model the surrounding structure,
2. stress field parameters near an each crack tip are calculated by the method of superposition of analytical and finite element solutions [7],
3. extensional lengths of cracks are calculated based on the Paris' law [8],
4. all cracks are extended along the predicted crack paths, and
5. go back to step1 to continue the simulation.

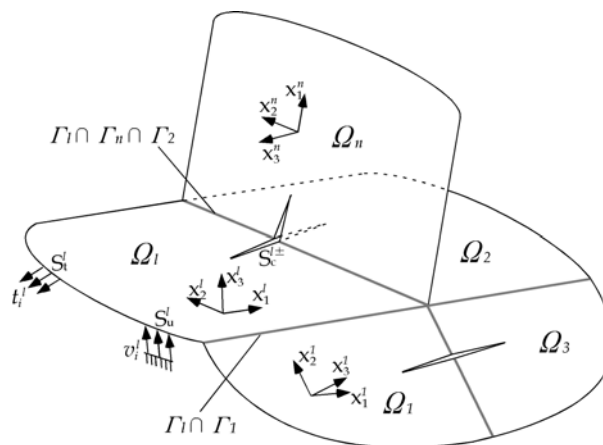


Figure 3 Cracks in a three-dimensional thin-plate structure.

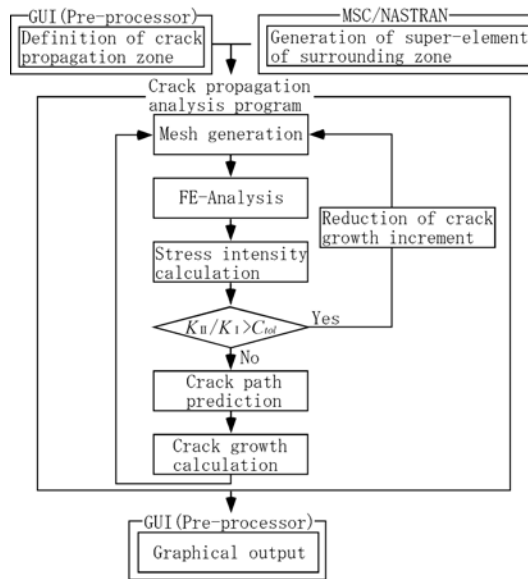


Figure 4 Flowchart of CP-System.

## SIMULATION OF FATIGUE CRACK PROPAGATION AT THE CONNECTION OF A LONGITUDINAL STIFFENER AND A TRANSVERSE GIRDER

In order to examine the fatigue crack propagation behavior at the intersection between longitudinal stiffeners and a transverse girder, numerical simulations of fatigue crack propagation were carried out by using the developed simulation program.

### *On the Effects of the Loading Conditions and the Structural Details*

An analysis model is illustrated in Fig.5, where it extends to 2 transverse spacing and 1.5 longitudinal spacing. In order to model the periodicity of the longitudinal stiffeners, symmetric conditions are prescribed along the both sides of the analysis model. The longitudinal stiffeners are connected to the transverse girder by a flat bar stiffener or a variety of brackets as illustrated in Fig.6 (a)-(d). We assumed either the water pressure loading condition or the axial loading condition, separately. In the case of the water pressure loading, uniform lateral pressure loading of constant amplitude is applied on the skin-plate, and the lateral displacement is restrained at the positions of the transverse girder. The longitudinal displacement is also restricted at the both ends. In the case of the axial loading condition, an axial force of constant amplitude is applied at the both ends of the model, and the lateral displacement is restrained at the positions of the transverse girder. The material properties of the analysis model are summarized in Table 1.

Figure 7 shows the finite element models. In the present simulation, it is assumed that the crack initiation point is fixed at the intersection of the face-plate and the end of the

web-stiffener. The initial crack is configured such that it has 40mm width in the face-plate and 10mm depth in the web plate, however, it should be noted that the plate thickness of the face-plate cannot precisely be taken into consideration within the framework of analysis by using shell elements. In the beginning of the simulation, crack-propagation domains are defined in the both parts of the face-plate and the web-plate. Having a crack reached the edge of the face-plate, the face-plate is treated as completely broken off, and the simulation continues by re-defining a single crack.

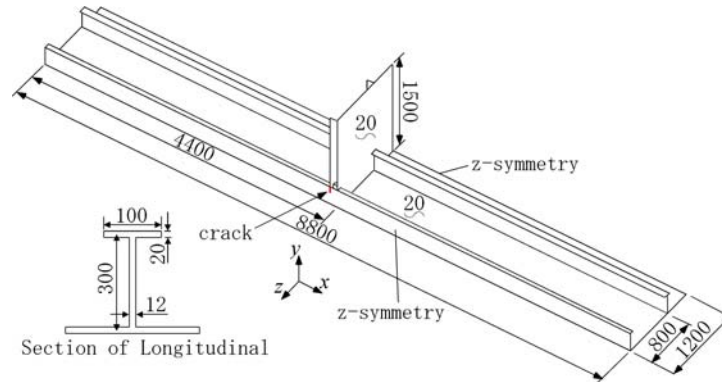


Figure 5 Analysis model of a stiffened panel.

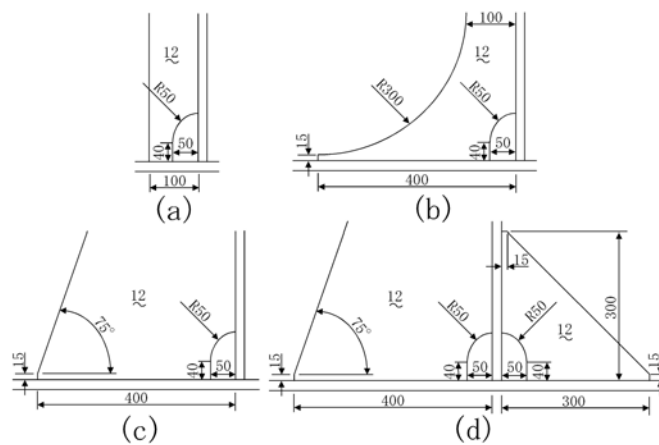


Figure 6 Structural details of web-stiffeners; (a) flat bar stiffener, (b) web-stiffener with rounded end, (c) large bracket, (d) large bracket with a back bracket.

Table 1 Material properties of the analysis model.

Young's modulus	206[GPa]
Poisson's ratio	0.3
threshold stress intensity range	2.9[MPa $\sqrt{m}$ ]
parameters for Paris' law	C=1.5 $\times 10^{-11}$ , m=2.75 [stress in MPa, length in m]

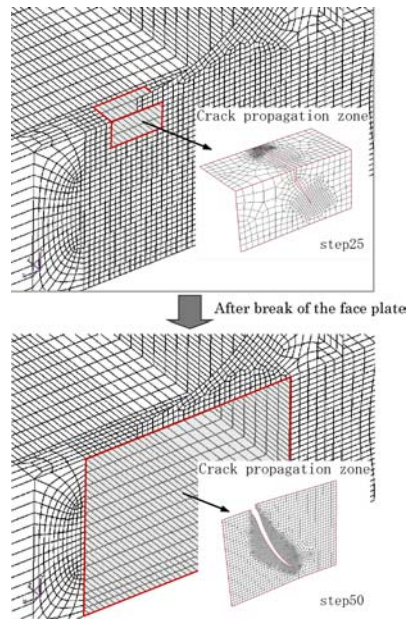


Figure 7 Finite element model.

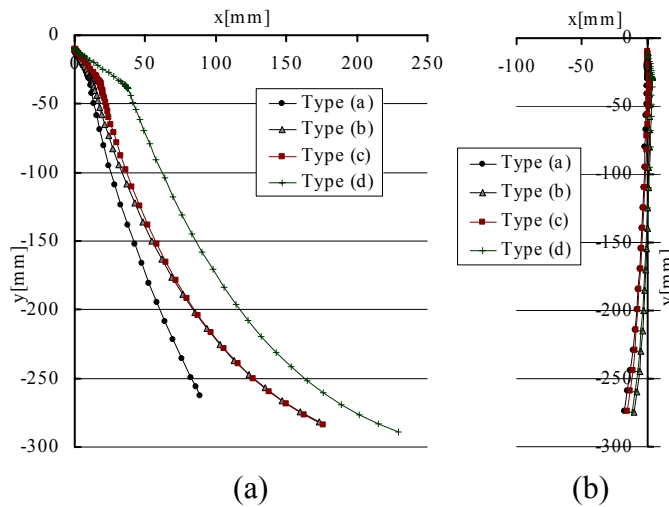


Figure 8 Simulated crack paths in the web-plate; (a) water pressure, (b) axial force.

The simulated crack paths in the web-plate are illustrated in Fig. 8, where the origins of coordinates are set at the intersections of the face-plate and the end of the web-stiffener. Under the water pressure loading, the cracks initiated from the end of web-stiffeners propagate toward the transverses girders. In the case of the structural details (b), (c) and (d), the cracks gradually curve and tend to avoid the penetration into the skin-plate. On the other hand, in the case of the structural detail (a), the crack tends to propagate towards the skin-plate, which may result in the failure of a compartment boundary. Under the axial force loading, the cracks tend to propagate towards the skin-plate regardless of the structural details.

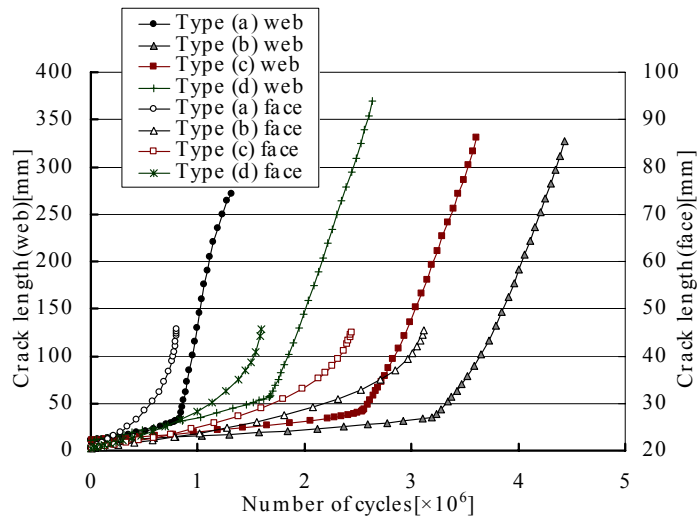


Figure 9 Simulated crack propagation lives under water pressure.

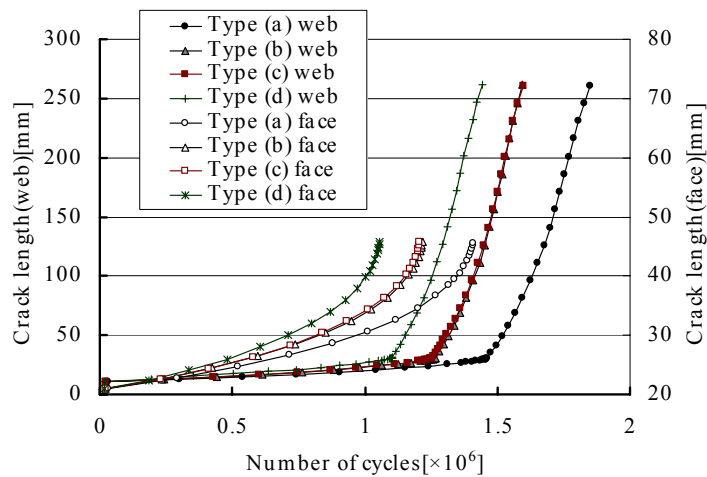


Figure 10 Simulated crack propagation lives under axial force.

In Fig. 9, the crack growth curves under the water pressure loading are illustrated. It is found that the crack propagation lives are significantly affected by the structural details. The difference of the crack propagation lives mainly occurs before the complete break-off of the face-plate. This difference of the crack propagation lives is caused by the difference of the nominal stress and/or the stress concentration at the initial crack of each model. In Fig.10, those under the axial force are illustrated, where the structural detail (a) exhibits the longest fatigue life, because the crack opening displacement may be strongly constrained compared to the other structural details due to the transverse girder.

#### ***On the Welding Residual Stress***

Since welding residual stress is not a fluctuating stress, we assume that it simply changes the stress ratio,  $R$ , and the effective ranges of stress intensity factor. In the

developed simulation program, the stress intensity factor contributed by the residual stress is separately calculated, and the actual stress intensity factor is obtained by the superposition of the stress intensity factors due to the applied load and the residual stress.

In order to investigate the effect of the residual stress against the fatigue crack propagation in the stiffened panel structures, a residual stress distribution is measured by using the test specimen, whose details are described in the following section (see Fig.14). The measured residual stress distribution is illustrated in Figs.11 and 12. Very high tensile residual stress appears along the fillet welds, and its counterbalancing compressive residual stress appears near the edges of the face-plate and in the middle part of the web-plate. The simulated crack propagation lives with and without residual stress are illustrated in Fig.13 for the structural detail (b). It is found that the crack propagation live before the break of the face-plate is considerably reduced by the effect of tensile residual stress. However, the fatigue crack is gradually retarded due to the effect of the compressive residual stress in the middle part of the web-plate, and it is almost arrested near the skin plate, which may be caused by the combined effects of the compressive residual stress and the structural redundancy.

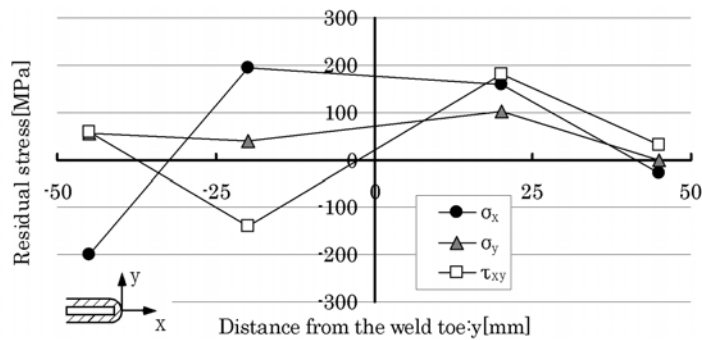


Figure 11 Measured residual stress distribution in the face-plate.

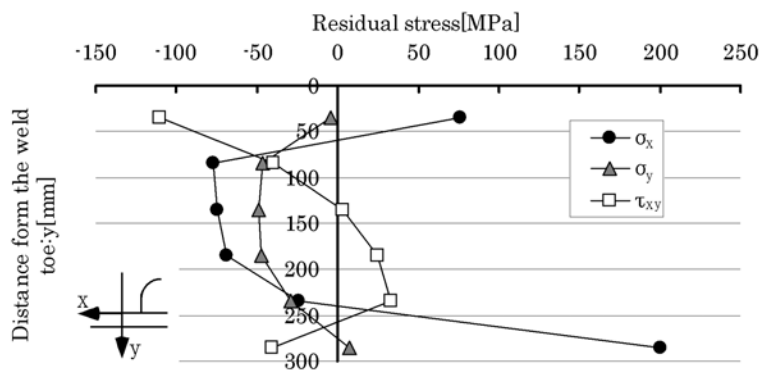


Figure 12 Measured residual stress distribution in the web-plate.

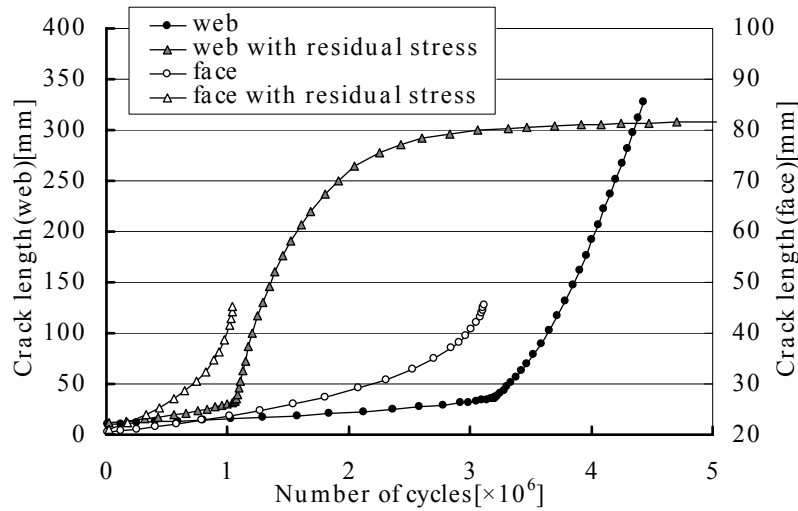


Figure 13 Simulated crack propagation lives considering the effect of residual stress.

## FATIGUE TESTS

### *Outline of the Tests*

Figure 14 is a schematic illustration of the fatigue tests. The material used is SM490A specified in JIS standard, whose material properties are shown in Table 2. The specimens are designed so that the applied stress, residual stress, and structural redundancy are equivalent to those attained in real ships. The specimens consist of three longitudinal stiffeners and a transverse girder at the middle span. The center longitudinal stiffener is connected to the transverse girder with a large bracket (the same dimensions as illustrated in Fig. 6(c)) or a flat bar stiffener (the same dimensions as illustrated in Fig.6(a)), where these specimens will be called as the bracket-type specimen and the stiffener-type specimen, respectively. A fatigue crack initiation is expected only at the intersection of the center longitudinal stiffener and the end of the web-stiffener. The loading condition is the three-point bending, and the applied hotspot stress range is set to 120MPa at the critical point. The repetition frequency of fatigue loading is set to 3~4Hz with the stress ratio, 0.05.

Table 2 Material properties of the specimen.

Tensile test					
thickness(mm)	Y. P. (N/mm <sup>2</sup> )	T. S. (N/mm <sup>2</sup> )		EL. (%)	
19	345	536		25	
12	361	529		26	
Chemical composition (%)					
thickness(mm)	C×100	Si×100	Mn×100	P×1000	S×1000
19	16	35	143	17	3
12	16	33	137	14	4

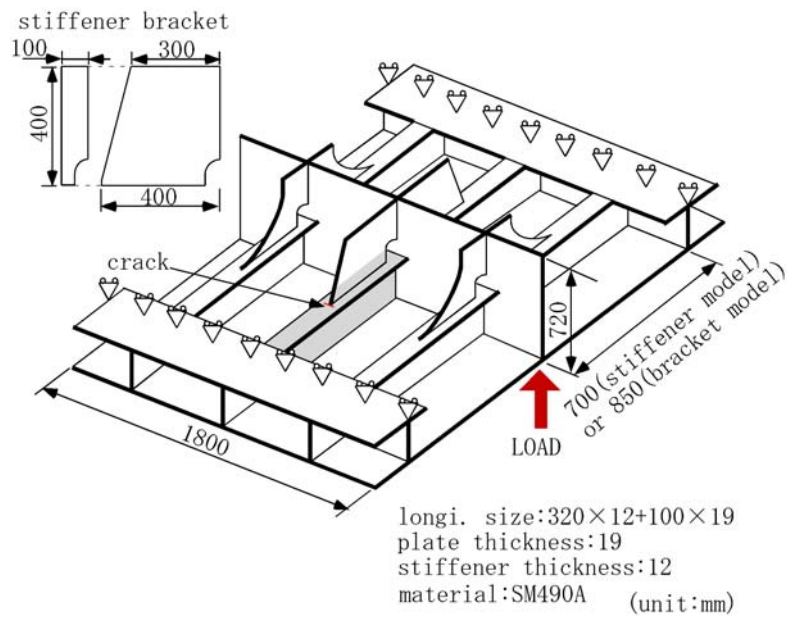


Figure 14 Test specimen

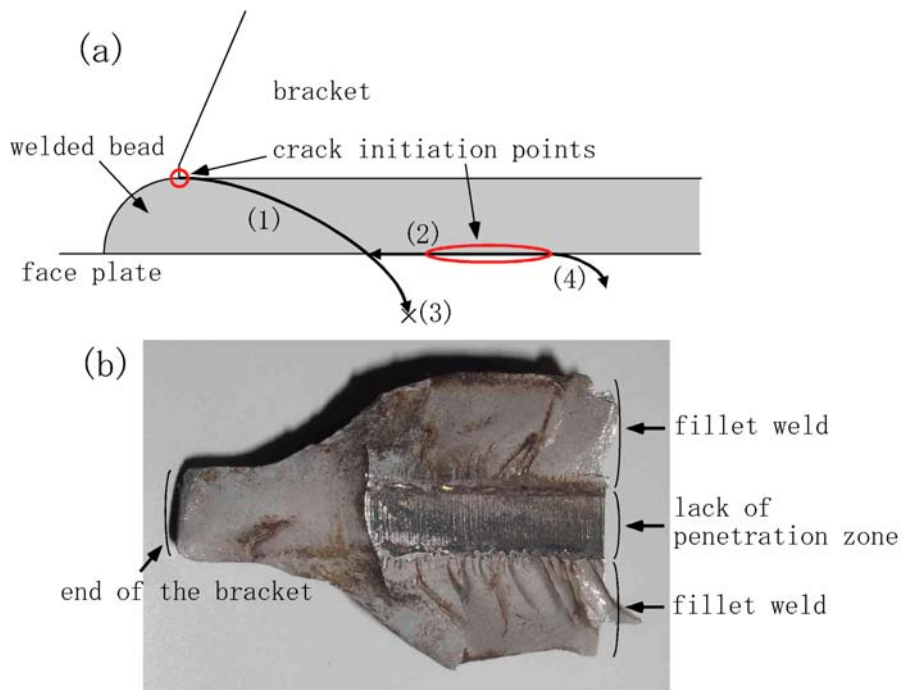


Figure 15 Crack propagation in the bracket-type specimen; (a) propagation behavior, (b) fracture surface.

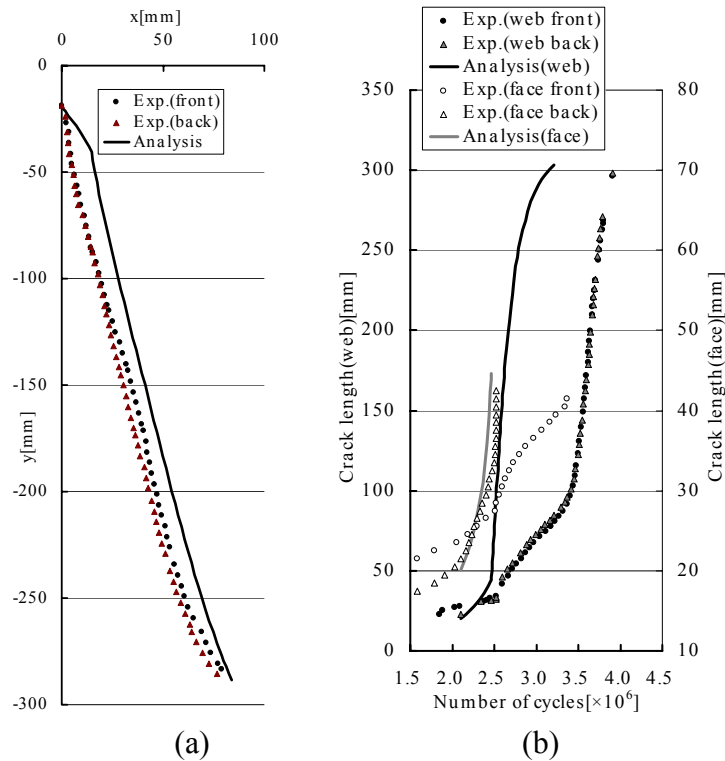


Figure 16 Comparison between experimental and analytical crack propagation of the stiffener-type specimen; (a) crack paths, (b) crack propagation lives.

### Test Results

The fatigue cracks in the bracket-type specimen exhibited the following behavior (see Fig. 15 (a));

- (1) a fatigue crack initiates at the end of the bracket, and propagates into the face-plate,
- (2) other cracks initiate from the weld root, and propagate to coalesce with the first crack,
- (3) the first crack is arrested in the face-plate, and
- (4) the secondary cracks propagate into the face-plate.

The experiment was stopped just after the step (4). From the observed crack growth behavior, it is inferred that the cracks may repeat the above process (2)-(4), so that they may result in the separation of the web-stiffener from the face-plate [9]. This crack growth behavior is quite different from the previous numerical simulation, but from the viewpoint of the ship structural safety, this sort of cracks may be favorable rather than those penetrating into the web-plate. Figure 15(b) shows the fracture surface of this specimen, where multiple fatigue cracks are initiated from the weld root, and their crack surfaces show some inclined angles. This may be due to the high out-of-plane shear stress with respect to the plane of the lack-of-penetration zone.

In the stiffener-type specimen, a fatigue crack was initiated at the weld toe of the face-plate, and propagated into the web-plate. In Figs. 16 (a) and (b), the crack paths and the crack growth curves are illustrated, respectively, where they are compared with

the numerical results. It can be seen that the fatigue crack in the experiment is slightly curved and propagates toward the shell plate, which is in good agreement with the simulated crack path. From Fig.16 (b), it can be seen that the fatigue cracks propagating in the face-plate exhibit asymmetric behavior. The reason may be the asymmetric residual stress distribution and/or the asymmetric loading caused by the welding deformation. On the experimental crack growth curve in the web-plate, the fatigue crack growth rate is rapidly increased at the two points,  $N=2.5 \times 10^6$  and  $N=3.5 \times 10^6$ , respectively, which correspond to the breaks of the each edge of the face-plate. The simulated crack growth curve also exhibits the similar phenomena except for the asymmetric crack growth behavior in the face-plate.

## CONCLUSIONS

From the numerical results, it has been found that the fatigue cracks from the intersection of the face-plate and the end of the web-stiffener may change their propagation behavior depending on the loading conditions and the structural details. In certain cases, the fatigue cracks show curved paths so as to avoid the penetration into the skin-plates, and they may be arrested in the web-plate because of the effect of the compressive residual stress. In the experiment of the bracket-type specimen, the fatigue failure occurred by root cracking, whose mode is the out-of- plane shear.

## Acknowledgements

This work has been in parts supported by the Program for Promoting Fundamental Transport Technology Research (Project No.2001-03) from Japan Railway Construction, Transport and Technology Agency (JRTT), and by Grant-in-Aid for Scientific Research (No.1720608600) from the Ministry of Education, Science and Culture to Yokohama National University. The authors are grateful for their support.

## REFERENCES

- 1 Sumi, Y., Mohri, M. and Kawamura, Y. (2005) *Fatigue Fract. Engng. Mater. Struct.* **28**, 107-115.
- 2 Sumi, Y. (1998) *J. Marine Science and Technology* **3-2**, 101-112.
- 3 Sumi, Y., Chen, Y. and Hayashi, S. (1996) *Int. J. Fracture* **82**, 205-220.
- 4 Sumi, Y., Chen, Y. and Wang, Z.N. (1996) *Int. J. Fracture* **82**, 221-235.
- 5 Sumi, Y. and Wang, Z.N. (1998) *Mechanics of Material* **28**, 197-206.
- 6 Kawamura, Y., Mu, Y. and Sumi, Y. (1999) *Trans. Japan Soc. Computational Enginng*; Paper No.19990024.
- 7 Yamamoto, Y. and Tokuda, N. (1973) *Int. J. Numer. Meth. Engng.* **6**, 427-439.
- 8 Kato, A., Kurihara, M., Kawahara, M. (1983) *J. Soc. Nav. Archit. Japan* **153**, 336-343 (in Japanese).
- 9 Doerk, O., Fricke, W. (2004) 9th Symposium on Practical Design of Ships and Other Floating Structures, Lubeck-Travemuende, Germany, 441-448.